Molecular Biology of the Cell
Vol. 19, 865–876, March 2008

Isc1p Plays a Key Role in Hydrogen Peroxide Resistance and Chronological Lifespan through Modulation of Iron Levels and Apoptosis

Teresa Almeida,*†‡ Marta Marques,*†‡ Dominik Mojzita,§ Maria A. Amorim,*† Rui D. Silva,‖ Bruno Almeida,¶ Pedro Rodrigues,* Paula Ludovico,¶ Stefan Hohmann,§ Pedro Moradas-Ferreira,*† Manuela Côrte-Real,‖ and Vítor Costa*†

*IBMC, Instituto de Biologia Molecular e Celular, Grupo de Microbiologia Celular e Aplicada, 4150-180 Porto, Portugal; †ICBAS, Instituto de Ciências Biomédicas Abel Salazar, Departamento de Biologia Molecular, Universidade do Porto, 4099-003, Porto, Portugal; §Department of Cell and Molecular Biology, Göteborg University, S-405 30 Göteborg, Sweden; ‖Departamento de Biologia-Centro de Biologia, Universidade do Minho, Campus de Gualtar, 4710-057 Braga, Portugal; and ¶Instituto de Investigação em Ciências da Vida e Saúde (ICVS), Escola de Ciências da Saúde, Universidade do Minho, Campus de Gualtar, 4710-057 Braga, Portugal

Submitted June 26, 2007; Revised December 11, 2007; Accepted December 19, 2007
Monitoring Editor: Donald Newmeyer

The inositolphosphosphingolipid phospholipase C (Isc1p) of *Saccharomyces cerevisiae* belongs to the family of neutral sphingomyelinases that generates the bioactive sphingolipid ceramide. In this work the role of Isc1p in oxidative stress resistance and chronological lifespan was investigated. Loss of Isc1p resulted in a higher sensitivity to hydrogen peroxide that was associated with an increase in oxidative stress markers, namely intracellular oxidation, protein carbonylation, and lipid peroxidation. Microarray analysis showed that Isc1p deficiency up-regulated the iron regulon leading to increased levels of iron, which is known to catalyze the production of the highly reactive hydroxyl radicals via the Fenton reaction. In agreement, iron chelation suppressed hydrogen peroxide sensitivity of *isc1*Δ mutants. Cells lacking Isc1p also displayed a shortened chronological lifespan associated with oxidative stress markers and aging of parental cells was correlated with a decrease in Isc1p activity. The analysis of DNA fragmentation and caspase-like activity showed that Isc1p deficiency increased apoptotic cell death associated with oxidative stress and aging. Furthermore, deletion of Yca1p metacaspase suppressed the oxidative stress sensitivity and premature aging phenotypes of *isc1*Δ mutants. These results indicate that Isc1p plays an important role in the regulation of cellular redox homeostasis, through modulation of iron levels, and of apoptosis.

INTRODUCTION

Sphingolipids have been considered as structural components of cellular membranes, but a number of recent studies revealed that ceramide and other bioactive sphingolipids play important roles in the regulation of various biological processes. In mammalian cells, ceramide is generated by acylation of a long-chain sphingoid base (LCB) derived from serine and palmitoyl-CoA or is produced by hydrolysis of complex sphingolipids through the action of sphingomyelinases. Both acid and neutral sphingomyelinases are activated in response to cellular stress, including ionizing radiation, DNA damage, heat stress, and oxidants. The resulting ceramide induce cellular responses ranging from apoptosis and cell cycle arrest to cell survival and proliferation (Hannun and Luberto, 2000). Recent studies suggest that ceramide formed via de novo biosynthesis or by the sphingomyelinase pathway play different regulatory functions (Jenkins *et al.*, 2002; Cowart *et al.*, 2006).

The LCB species of *Saccharomyces cerevisiae* and mammalian cells are similar but yeast cells use ceramide to synthesize inositolphosphosphingolipids, such as inositolphosphoceramide (IPC), mannose-IPC (MIPC), and $M(IP)_2C$, instead of sphingomyelin (reviewed in Le Stunff *et al.*, 2002). These complex sphingolipids are hydrolyzed by Isc1p, an inositolphosphosphingolipid-phospholipase C. Isc1p also has neutral sphingomyelinase activity and has 30% identity to mammalian neutral sphingomyelinase (nSMase2). Isc1p and nSMase2 share other common features, as both require Mg^{2+} for optimal activity, are activated selectively by anionic phospholipids, such as phosphatidylserine, cardiolipin, and phosphatidylglycerol, and contain a P-loop-like domain that seems to be essential for catalysis and Mg^{2+}

This article was published online ahead of print in *MBC in Press* (http://www.molbiolcell.org/cgi/doi/10.1091/mbc.E07–06–0604) on December 27, 2007.

‡ These authors contributed equally to this work.

Address correspondence to: Vítor Costa (vcosta@ibmc.up.pt).

Abbreviations used: ROS, reactive oxygen species; BPS, bathophenanthroline disulfonic acid; LCB, long-chain sphingoid base; H_2DCFDA, 2′,7′-dichlorodihydrofluorescein diacetate; MDA, malondialdehyde.

Table 1. *Saccharomyces cerevisiae* strains used in this study

Strain	Genotype	Reference/source
BY4741	Matα, *his3*Δ_1, *leu2*Δ_0, *met15*Δ_0, *ura3*Δ_0	EUROSCARF
yca1Δ	[BY4741] *yca1*Δ*::KanMx4*	EUROSCARF
BY4741 pYES2	[BY4741] pYES2*::URA3*	This study
BY4741 p*ISC1*	[BY4741] pYES2-*ISC1*:: *URA3*	This study
BY4741 *CTH2*-LacZ	[BY4741] pCM64-*CTH2*-FeRE-*CYC1*-LacZ	This study
BY4741 *CTH2*-LacZ M3	[BY4741] pCM64-*CTH2*-FeRE-*CYC1*-LacZ M3	This study
isc1Δ	[BY4741] *isc1*Δ*::KanMx4*	EUROSCARF
isc1Δ*yca1*Δ	[BY4741] *isc1*Δ*::KanMx4 yca1*Δ:: *URA3*	This study
Isc1Δ p*ISC1-FLAG*	[*isc1*Δ] pYES2-*ISC1-FLAG*:: *URA3*	This study
isc1Δ *CTH2*-LacZ	[*isc1*Δ] pCM64-*CTH2*-FeRE-*CYC1*-LacZ	This study
isc1Δ *CTH2*-LacZ M3	[*isc1*Δ] pCM64-*CTH2*-FeRE-*CYC1*-LacZ M3	This study

binding (Okamoto *et al.*, 2002; Sawai *et al.*, 2000). During exponential growth, Isc1p localizes to the endoplasmic reticulum, but it is posttranslationally activated in the postdiauxic phase by translocation into mitochondria (Vaena de Avalos *et al.*, 2004). The activation of Isc1p is dependent on Pgs1p, which catalyzes the committed step in the synthesis of phosphatidylglycerol and cardiolipin in the mitochondria. Loss of either *ISC1* or *PGS1* results in down-regulation of the mitochondrial cytochrome c oxidase subunits Cox3p and Cox4p, suggesting that Isc1p mediates at least some functions downstream of phosphatidylglycerol/cardiolipin (Ostrander *et al.*, 2001; Vaena de Avalos *et al.*, 2005).

Recent studies suggest a link between changes in sphingolipid metabolism, oxidative stress resistance, and lifespan in yeast. The Lag1 ceramide synthase plays a key role in replicative longevity by modulating metabolism and stress resistance (Jiang *et al.*, 2004). The *LAG1* as well as other genes associated with sphingolipid metabolism, namely *YPC1*, *YSR3*, *LCB5*, and *IPT1*, are differentially expressed in aged and apoptotic cells (Laun *et al.*, 2005). In addition, the *ipt1*Δ mutants lack $M(IP)_2C$ and are more resistant to oxidative stress and have an increased chronological lifespan, whereas yeast mutants with increased levels of $M(IP)_2C$ are hypersensitive to oxidative stress and display a shorter lifespan (Aerts *et al.*, 2006).

In this study, we investigated the role of the yeast Isc1p in oxidative stress resistance and chronological lifespan in the yeast *S. cerevisiae*. The results indicate that Isc1p deficiency increased hydrogen peroxide–induced cell death and cellular senescence by an apoptotic mechanism associated with higher levels of oxidative stress markers. Our results also implicate Isc1p in the regulation of iron homeostasis and suggest that the oxidative stress hypersensitivity of Isc1p-deficient mutants may result from an increased production of the highly reactive hydroxyl radicals catalyzed by iron (Fenton reaction).

MATERIALS AND METHODS

Yeast Strains, Plasmids, and Growth Conditions

The strains of *S. cerevisiae* used in this study are listed in Table 1. Wild-type (BY4741) and *isc1*Δ cells were grown in YPD (1% (wt/vol) yeast extract, 2% (wt/vol) bactopeptone, and 2% (wt/vol) glucose) to early exponential phase (OD_{600} = 0.6), or to postdiauxic-shift phase (OD_{600} = 10 for BY4741; OD_{600} = 6 for *isc1*Δ mutants), in an orbital shaker, at 26°C, and 120 rpm, with a ratio of flask volume/medium volume of 5:1. For *YCA1* disruption, a deletion fragment containing *URA3* and the flanking regions of *YCA1* was amplified by PCR using pYES2 and the following primers: F (GACCGACTAGATTTACAATCATGTATCCAGGTAGTGGACGTGGTAATAACTGATATAATT) and R (ACGTACACATTCATATATTTCTACATAATAAATTGCAGATTTTGATTCCGGTTTCTTTGA). Yeast strains were transformed by electroporation. Gene disruption was confirmed by PCR analysis and Southern blotting. For *ISC1* overexpression, *S. cerevisiae* BY4741 cells were transformed with *GAL1*-promoter driven pYES2 (empty vector) or pYES2-*ISC1* (kindly provided by Dr. Y. Hannun, Medical University of South Carolina). For expression of FLAG-tagged Isc1p, *isc1*Δ cells were transformed with pYES2-*ISC1-FLAG*. Transformed cells were grown in minimal medium-GAL (0.67% [wt/vol] yeast nitrogen base without amino acids, 2% [wt/vol] galactose) supplemented with appropriate amino acids (40 mg histidine l^{-1}, 80 mg leucine l^{-1}, 40 mg methionine l^{-1}). Plasmids containing consensus (pCM64-*CTH2*-FeRE-*CYC1*-LacZ) or mutant (pCM64-*CTH2*-FeRE-*CYC1*-LacZ M3) Aft1 binding sequences from *CTH2* promoter fused to the *CYC1* minimal promoter-LacZ reporter (Puig *et al.*, 2005) were a generous gift from Dr. D. Thiele (Duke University Medical Center, Durham, NC). BY4741 and *isc1*Δ cells expressing the *CTH2*-LacZ or *CTH2*-LacZ M3 were grown in minimal medium-GLC (0.67% (wt/vol) yeast nitrogen base without amino acids, 2% (wt/vol) glucose) supplemented with appropriate amino acids (40 mg histidine l^{-1}, 80 mg leucine l^{-1}, 40 mg methionine l^{-1}).

Oxidative Stress and Chronological Lifespan Assay

For the analysis of oxidative stress resistance, yeast cells were grown to exponential phase (OD_{600} = 0.6) and treated with H_2O_2 for 1 h. To test the effect of iron deprivation on H_2O_2 resistance, cells were grown to exponential phase and preincubated with 20 μM bathophenanthroline disulfonic acid (BPS) for 4 h. Control and treated cells were diluted in YPD medium and plated on YPD medium containing 1.5% agar (150–180 cells/plate). Colonies were counted after growth at 26°C for 3 d. Viability was expressed as the percentage of the colony-forming units. Chronological lifespan was assayed as previously described (Harris *et al.*, 2003). Cells were centrifuged at 4,000 rpm for 5 min, washed twice with water, resuspended in water, and incubated at 26 or 37°C for the indicated times. Viability was determined as described for H_2O_2 stress.

Protein Carbonylation, Lipid Peroxidation and Intracellular Oxidation

Protein oxidation was determined by immunodetection of protein carbonyls, as previous described (Costa *et al.*, 2002). Protein content of cellular extracts was estimated by the method of Lowry, using bovine serum albumin as a standard. Protein carbonylation assays were performed by slot blot analysis using rabbit IgG anti-DNP (Dako, Glostrup, Denmark) at a 1:5,000 dilution, as primary antibody, and goat anti-rabbit IgG-peroxidase (Sigma, St. Louis, MO) at a 1:5,000 dilution, as secondary antibody. Immunodetection was performed by chemiluminescence, using a kit from Amersham (RPN 2109). Quantification of carbonyls was performed by densitometry. Lipid peroxidation was determined by quantifying thiobarbituric acid reactive substances, as described (Belinha *et al.*, 2007) and expressed as nmol MDA (mg protein)$^{-1}$. The oxidant-sensitive probe 2′,7′-dichlorodihydrofluorescein diacetate (H_2DCFDA) was used to measure the levels of intracellular oxidation (Davidson *et al.*, 1996). Fluorescence was measured using a spectrofluorimeter set at an excitation wavelength of 504 nm and an emission wavelength of 524 nm. H_2DCFDA (10 μM) was added to the culture and incubated for 15 min to allow uptake of the probe. Cells untreated or exposed with H_2O_2 and aged cells were cooled on ice, harvested by centrifugation, and washed twice with 50 mM phosphate buffer, pH 6.0. The cell pellets were resuspended in 500 μl of the same buffer and lysed by vortexing in the presence of glass beads. Protein concentration was determined in supernatants obtained after centrifugation at 13,000 rpm for 5 min. Fluorescence was measured using 5 μg protein. Unlabeled controls were prepared and autofluorescence was subtracted.

Northern Blot and Microarray Analysis

RNA was isolated by the acid phenol method as described by Ausubel *et al.* (1998). For Northern blot analysis, total RNA (30 μg) was denatured with glyoxal and dimethyl sulfoxide, blotted onto Hybond N membranes, and probed as described by Sambrook *et al.* (1989). The following probes were used: a 1-kb HindIII-EcoRI fragment of *ACT1* gene, a 1.5-kb BglII-BglII fragment of *SSA4* gene, a 1.5-kb BglII-PstI fragment of *HSP26* gene, a 1.1-kb EcoRI-EcoRI fragment of *CTT1* gene, a 0.5-kb HindIII- HindIII fragment of *SOD1* gene and a 470-base pair BglII-BglII fragment of *SOD2* gene. *ACT1* gene was used as RNA loading control. Band intensities were evaluated by densitometry. For microarray analysis, the synthesis of ^{33}P-CTP-labeled cDNA and the hybridization, washing, and stripping of Genefilters (Research Genetics, Huntsville, AL) were performed as described previously (Rep *et al.*,

2000). A Molecular Imager FX (Bio-Rad, Richmond, CA) was used to obtain a digital image of the filters. Images were converted to TIFF and imported into the Pathways4 Software (Research Genetics). Pathways4 was used to compare gene filter images. Before determination of induction or repression of gene expression, all spot intensities were normalized, by dividing sampled intensities by the mean sampled intensities of all clones. To determine the -fold induction or repression, the relative mRNA level was expressed as the ratio *isc1*Δ mutant/wild-type cells. Genes that changed at least twofold by *ISC1* disruption were considered for further analysis. All values are means of the expression profiles of four experiments with similar results, using independent cultures grown under the same conditions. Statistical analysis of the microarray data was performed by using BRB ArrayTools (version 3.3.0 beta 1) developed by Dr. Richard Simon and Amy Peng Lam (http://linus.nci.nih.gov/BRB-ArrayTools.html). The data were deposited in the microarray data public repository ArrayExpress (http://www.ebi.ac.uk/miamexpress/; Parkinson *et al.*, 2005) under the accession number E-MEXP-1136. Statistical analysis of overrepresentation of functional groups was performed by using FUNSPEC (Robinson *et al.*, 2002). All available databases were addressed by using a probability cutoff of $1e^{-4}$ and the Bonferroni correction for multiple testing.

Iron Levels

Yeast cells (5×10^8) were washed twice with H_2O, resuspended in 0.5 ml of 3% (vol/vol) nitric acid, and incubated 16 h at 98°C. The supernatant (400 μl) was mixed with 160 μl of 38 mg sodium ascorbate ml^{-1}, 320 μl of 1.7 mg BPS ml^{-1} (ethanol:chloroform, 2:1), and 126 μl of ammonium acetate (saturated solution diluted 1:3). The organic phase was diluted 20-fold in ethanol: chloroform (2:1), and the absorbance was measured at 535 nm. Iron was quantified by reference to a standard curve using iron sulfate (Tamarit *et al.*, 2006).

Glutathione Determination

Yeast extracts were prepared as described (Belinha *et al.*, 2007), and glutathione was assayed by the method of Tietze (1969). The rate of color development was monitored at 405 nm. The concentration was determined by reference to a GSSG standard added to the assay cuvette (internal standard) and was expressed as nmol glutathione $(\mu g \text{ protein})^{-1}$.

Enzymatic Activities

For superoxide dismutase and catalase activity, yeast extracts were prepared in 50 mM potassium phosphate buffer (pH 7.0) and proteases inhibitors, by vigorous shaking of the cell suspension, in the presence of glass beads, for 5 min. Short pulses of 1 min were used, with 1-min intervals on ice. Protein content was estimated as described above. Proteins were separated by native PAGE, using 60 μg protein. Superoxide dismutase activity was determined in situ, as described by Flohé and Otting (1984). MnSOD activity was detected in the presence of 2 mM potassium cyanide. Catalase activity was analyzed in situ, in the presence of 3,3′-diaminobenzidine tetrahydrochloride, using the H_2O_2/peroxidase system (Conyers and Kidwell, 1991). For sphingomyelinase activity, yeast extracts were prepared in 25 mM Tris (pH 7.4), 5 mM EDTA, and 1 mM PMSF and cleared by centrifugation at 3000 rpm for 10 min. The supernatant was further centrifuged at 13,000 rpm for 1 h. The pellet was ressuspendend in 25 mM Tris (pH 7.4), 5 mM EDTA, and 1 mM PMSF and used for the assay. The protein concentration was measured by the Lowry method, and neutral sphingomyelinase activity was determined by using the Amplex Red Sphingomyelinase Assay Kit (Molecular Probes, Eugene, OR). The fluorescence intensity was measured at 590 nm (excitation at 560 nm) with a multiwell plate reader (Spectra MAX Gemini XS, Molecular Devices, Menlo Park, CA) and temperature-controlled to 37°C. For the β-galactosidase assay, yeast cells expressing consensus or mutant Aft1-LacZ reporter were grown in minimal medium to exponential phase and treated with 20 μM BPS for 4 h. The β-galactosidase activity was measured as previously described (Ausubel *et al.*, 1998), with the following modification: a cellular extract prepared, as described above, in 100 mM Tris-HCl, 1 mM DTT, 10% (vol/vol) glycerol, and 40 μg of total protein was used in the assay.

Analysis of Apoptotic Markers

DNA strand breaks were detected by terminal deoxynucleotidyl transferase–mediated dUTP nick end labeling (TUNEL), using the "In situ cell death detection kit, fluorescein" (Boehringer Mannheim, Indianapolis, IN). A protocol modified from Ludovico *et al.* (2001) was used. Cells were fixed with 3.7% (vol/vol) formaldehyde and applied to poly-lysine–coated slides. Cell wall was digested with lyticase, and the slides were rinsed with PBS, incubated in permeabilization solution (0.1% (vol/vol) Triton X-100, 0.1% (wt/vol) sodium citrate) for 2 min on ice, rinsed twice with PBS, and incubated with 40 μl TUNEL reaction mixture, containing terminal deoxynucleotidyl transferase and FITC-dUTP, for 60 min at 37°C. The slides were rinsed two times with PBS and incubated for 20 min with 40 μl of 50 mg propidium iodide (PI) ml^{-1} and 12.5 mg RNase ml^{-1} solution. Slides were rinsed three times with PBS, and a coverslip was mounted with a drop of antifading agent Vectashield (Molecular Probes). For image acquisition, an Olympus BX61 microscope (Melville, NY) with filter wheels to control excitation and emission wavelength, equipped with a high-resolution DP70 digital camera and DP Manager Software was used. For the quantitative assessment of TUNEL staining, 150–700 cells were counted per sample.

Caspase-like or ASPase activity was detected using a CaspSCREEN Flow Cytometric Analysis Kit (Chemicon, Temecula, CA) essentially as described before (Almeida *et al.*, 2007). Cells were incubated with the nonfluorescent substrate D_2R [$(Asp)_2$-rhodamine 110] at 37°C for 90 min and then analyzed by flow cytometry. Flow cytometry analysis was performed on an EPICS XL-MCL (Beckman-Coulter, Hialeah, FL) flow cytometer, equipped with an argon-ion laser emitting a 488-nm beam at 15 mW. The green fluorescence was collected through a 488-nm blocking filter, a 550-nm long-pass dichroic filter, and a 525-nm bandpass filter. Twenty thousand cells per sample were analyzed. The data were evaluated with the MULTIGRAPH software included in the system II acquisition software for the EPICS XL/XL-MCL version 1.0 (Beckman-Coulter).

Statistical Analysis

Data are expressed as mean values ± SD of at least three independent experiments. Values were compared by Student's *t* test. The 0.05 probability level was chosen as the point of statistical significance throughout.

RESULTS

Hydrogen Peroxide Sensitivity of isc1Δ Mutant Cells

Several previous studies suggested that sphingolipid metabolism plays an important role in redox homeostasis (Won and Singh, 2006). Aiming at investigating the role of the yeast homologue of mammalian neutral sphingomyelinase (Isc1p) during oxidative stress, *S. cerevisiae isc1*Δ mutant strain and its isogenic BY4741 parental strain were grown to the exponential phase and exposed to H_2O_2. Analysis of cellular viability showed that cells deficient in Isc1p were hypersensitive to H_2O_2: 5% of *isc1*Δ mutant cells remained viable after 1 h exposure to 1.5 mM H_2O_2, whereas 26% of wild-type cells survived (Figure 1A). To study oxidative stress resistance of cells overexpressing *ISC1*, *S. cerevisiae* BY4741 cells were transformed with pYES2 (empty vector) or pYES2-*ISC1* (gene expression under the *GAL1*- promoter) and grown in minimal medium with 2% galactose. Cells grown in this medium were considerably more resistant to H_2O_2. Therefore, we used 10 mM H_2O_2 in these experiments. The data show that *ISC1* overexpression did not increase oxidative stress resistance (Figure 1B).

In yeast, as in other cell types, an oxidative stress response is triggered when cells are exposed to low concentrations of H_2O_2, leading to the acquisition of cellular resistance to a subsequent lethal stress (Godon *et al.*, 1998). The deficiency in Isc1p did not impair the acquisition of oxidative stress resistance by pre-exposure of exponential phase cells to 0.4 mM H_2O_2 for 30 min before 1.5 mM H_2O_2 treatment: in the BY4741 strain, cellular viability increased from 26 ± 4 to 49 ± 6%, whereas in *isc1*Δ mutants it increased from 5 ± 2 to 24 ± 2%. Postdiauxic phase cells are also known to display an intrinsically higher stress resistance. The H_2O_2 resistance of both parental and *isc1*Δ mutant cells also increased by growth from the exponential to the postdiauxic shift phase: 57 ± 14% of *isc1*Δ mutant cells remained viable after 1 h exposure to 5 mM H_2O_2, whereas 84 ± 15% of BY4741 cells survived. In all cases, *isc1*Δ mutant cells were always more sensitive to H_2O_2.

Hydrogen peroxide promotes intracellular oxidation and induces DNA damage, lipid peroxidation, and protein carbonylation (Cabiscol *et al.*, 2000; Costa *et al.*, 2002). Therefore, we investigated if the higher sensitivity of *isc1*Δ mutant cells was associated with higher levels of oxidative stress markers, such as intracellular oxidation, protein carbonylation, and lipid peroxidation. Intracellular oxidation was determined using a molecular probe that is sensitive to reactive oxygen species (ROS), H_2DCFDA. The results show that

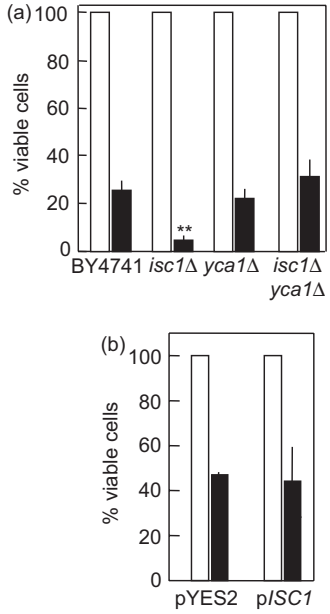

Figure 1. Role of Isc1p in hydrogen peroxide resistance. (a) *S. cerevisiae* BY4741, *isc1*Δ, *yca1*Δ, and *isc1*Δ*yca1*Δ mutant cells were grown in YPD medium to the exponential phase (OD_{600} = 0.6) and exposed to 1.5 mM H_2O_2 for 1 h. (b) *S. cerevisiae* BY4741 transformed with pYES2 or pYES2-*ISC1* were grown in minimal medium with 2% galactose and treated with 10 mM H_2O_2 for 1 h. Controls (□) and treated cells (■) were plated on YPD 1.5% agar medium. Cell viability was expressed as the percentage of the colony-forming units (treated cells vs. nonstressed cells). Values are means ± SD of three independent experiments. **$p < 0.01$.

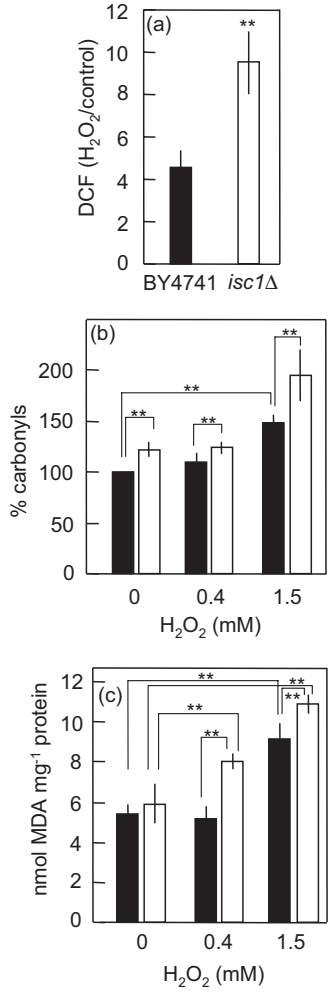

Figure 2. Effect of hydrogen peroxide on intracellular oxidation and oxidative damages. *S. cerevisiae* BY4741 (■) and *isc1*Δ mutant (□) cells were grown to exponential phase and treated with H_2O_2 for 60 min. (a) Intracellular oxidation. Cells were labeled with the molecular probe H_2DCFDA and lysed as described in *Materials and Methods*. Data are expressed as the fluorescence ratio between 1.5 mM H_2O_2-treated and untreated cells. (b) Protein carbonylation. Proteins were derivatized with DNPH and slot-blotted into a PVDF membrane. Immunodetection was performed using an anti-DNP antibody, as described in *Materials and Methods*. Quantitative analysis of total protein carbonyl content was performed by densitometry using data taken from the same membrane. (c) Lipid peroxidation. Cellular extracts were prepared, and MDA was determined as described in *Materials and Methods*. Values are means ± SD of three independent experiments. **$p < 0.01$.

intracellular oxidation induced by H_2O_2 (1.5 mM, 1 h) was 2.1-fold higher in cells lacking Isc1p, compared with parental cells (Figure 2A). In agreement, under the same conditions, H_2O_2-induced protein carbonylation increased in *isc1*Δ mutant cells (195%), compared with parental cells (148%). Notably, *isc1*Δ mutant cells showed a small but statistically significant increase in constitutive carbonyl levels (122% of the observed in parental cells) (Figure 2B). The analysis of lipid peroxidation showed similar constitutive levels in the *isc1*Δ mutant and parental cells (Figure 2C). However, lipid peroxidation levels increased to 136% in *isc1*Δ cells treated with 0.4 mM H_2O_2, a concentration that did not affect parental cells. Furthermore, the induction of lipid peroxidation by exposure to 1.5 mM H_2O_2 was higher in *isc1*Δ mutant cells (185% compared with 168% for parental cells). The overall results suggest that Isc1p-deficient cells exhibit a lower resistance to H_2O_2 associated with an increased accumulation of oxidized proteins and lipids, exceeding the levels assessed in parental cells, because of a higher intracellular oxidation.

Transcriptome Analysis in isc1Δ Mutant Cells

Antioxidant defenses and stress proteins play critical roles in cellular protection against oxidative damages (Costa and Moradas-Ferreira, 2001). Aiming to identify genes differentially expressed in Isc1p-deficient cells, we initially analyzed both constitutive and H_2O_2-induced mRNA levels of some antioxidant defense genes (*SOD1*, Cu,Zn-superoxide dismutase; *SOD2*, Mn-superoxide dismutase; *CTT1*, cytosolic catalase) and heat-shock proteins (*HSP26* and *SSA4*, a HSP70 family member). These genes were selected based on the fact that different transcription factors control their induction under oxidative stress. Yap1p and Skn7 regulate *SOD1* and *SOD2*, whereas Msn2/4p controls the expression of *CTT1*, *HSP26*, and *SSA4*. Isc1p deficiency did not affect the constitutive expression of these genes or impaired their induction in response to 0.4 mM H_2O_2 (Supplementary Figure S1). These results suggest that the higher sensitivity of *isc1*Δ mutant cells to H_2O_2 is not due to lower levels of these antioxidant defenses or heat-shock proteins.

To characterize global changes in the transcriptome of *isc1*Δ mutant cells, a microarray study was performed. The deficiency in Isc1p led to an increase of the mRNA levels of 72 genes, whereas that of 146 genes (including 75 encoding ribosomal proteins) was diminished (see Supplementary Ta-

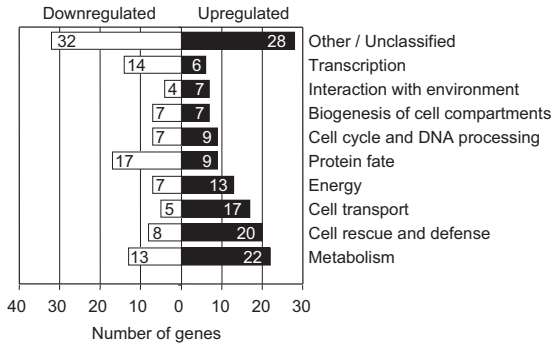

Figure 3. Functional categories of genes differentially expressed in *isc1*Δ mutant cells. *S. cerevisiae* BY4741 and *isc1*Δ mutant cells were grown to exponential phase, and RNA was isolated as described in *Materials and Methods.* Whole changes in the transcriptome were analyzed using Genefilters (Research Genetics). Genes up- or down-regulated in *isc1*Δ cells were sorted in groups according to Munich Information Center for Protein Sequences (MIPS) database. Down-regulated genes associated with protein biosynthesis (n = 87) were not included. See Supplementary Table S1 for all data.

ble S1). Genes differentially expressed were sorted into functional categories according to MIPS. Although these genes are associated with diverse functions, our data show that some categories are significantly more represented in *isc1*Δ mutant cells compared with wild-type cells (Figure 3): genes associated with protein biosynthesis (66%) and protein fate (12%) were down-regulated, whereas genes related with cell rescue, defense and virulence (28%), cell transport, transport facilitation, and transport routes (24%) were up-regulated by *ISC1* disruption.

To identify biological processes overrepresented, gene lists were analyzed by using the FUNSPEC software (Robinson *et al.,* 2002). The most important cellular functions induced include those associated with carbohydrate metabolism, cell rescue and defense, iron uptake, and cell wall (Table 2). Most of the genes related with carbohydrate metabolism (*HXK1*, *GLK1*, *TDH1*, *TDH3*, *PGK1,* and *ENO1*) were associated with the glycolytic pathway. Disruption of the *ISC1* gene also increased the expression of *PDR5*, which encodes an ABC drug efflux pump, which is important for cellular detoxification (Mamnun *et al.,* 2004), and *PUP2,* which encodes a subunit of the 20S proteasome, which is involved in the degradation of oxidized proteins (Inai and Nishikimi, 2002; Shringarpure *et al.,* 2003). Several genes up-regulated in the *isc1*Δ mutant cells that were associated with cell rescue and defense encode cell wall proteins (Table 2), namely *TIR2-4,* which are induced under anaerobic conditions (Abramova *et al.,* 2001), and *YGP1,* which is induced by nutrient starvation (Destruelle *et al.,* 1994), as well as proteins involved in cell wall stress signal transduction (*MTL1*) or cell wall biogenesis (*GSC2* and *ROM1*; see Supplementary Table S1). The up-regulation of *YGP1* and *PDR5* in cells lacking Isc1p was also observed in another yeast strain (Cowart *et al.,* 2006). Interestingly, loss of Isc1p increased the expression of six genes associated with iron uptake: *FIT2* and *FIT3* gene products are involved in the retention of siderophore-iron in the cell wall; *ARN1*, *ARN2*, *ARN3/SIT1,* and *ARN4/ENB1* encode transporters of siderophore-iron (Kosman, 2003).

Isc1p Deficiency Increase Iron Levels

Iron uptake genes are up-regulated under iron deprivation conditions (Philpott *et al.,* 2002). However, the induction of these genes in iron replete medium may lead to iron overload. Thus, we investigated if iron levels were altered in *isc1*Δ mutant cells. The results show that Isc1p deficiency increased iron levels 50% in the exponential phase, when compared with the parental strain (Figure 4A). This increase was even higher (3–4-fold) in the postdiauxic phase. In both parental and *isc1*Δ cells, iron content increased during growth from the exponential to the postdiauxic phase.

Iron overload in mitochondria of cells lacking frataxin, a yeast model of Friedreich ataxia, results in MnSOD deficiency and increases oxidative stress sensitivity (Desmyter *et al.,* 2004; Irazusta *et al.,* 2006). However, the analysis of MnSOD showed that its activity was similar in parental and *isc1*Δ cells (Figure 4B). Thus, it seems unlikely that excess iron in *isc1*Δ cells accumulates within mitochondria.

The Aft1p transcription factor is a key regulator of the iron regulon (Rutherford *et al.,* 2005). Under iron-sufficient conditions, Aft1p remains inactive because of its cytoplasmic localization. It was recently shown that the nuclear monothiol glutaredoxins Grx3p and Grx4p are critical for iron inhibition of Aft1p (Ojeda *et al.,* 2006). Notably, our microarray analysis showed that *GRX3* gene expression decreases in *isc1*Δ mutants (see Supplementary Table S1). To investigate

Table 2. Functional categories overrepresented in the microarray data of *isc1*Δ mutants

Up-regulated		
Database/Annotation	p-value	Genes in category from cluster
MIPS functional classification		
Glycolysis and gluconeogenesis	$2.14e^{-06}$	*GLK1 PGK1 HXK1 TDH3 ENO1 TDH1*
Cell rescue, defense and virulence	$5.61e^{-05}$	*SIT1 PUP2 ARN1 ARN2 TIR3 GTT1 YGP1 ENB1 YOL161C TIR4 TIR2 PDR5*
GO Biological Process		
Siderochrome transport	$2.23e^{-07}$	*SIT1 ARN1 ARN2 ENB1*
Carbohydrate metabolism	$8.97e^{-05}$	*GLK1 PGK1 HXK1 GSC2 TDH3 ENO1 TDH1 TSL1 IDH2*
GO Cellular Component		
Cell wall	$7.92e^{-06}$	*BGL2 TIR3 SIM1 YGP1 TIR4 TIR2 FIT2 FIT3*
Down-regulated		
Database/Annotation	p-value	Genes in category from cluster
MIPS Functional Classification		
Ribosome biogenesis	$1.00e^{-14}$	78 genes
GO Biological Process		
Protein biosynthesis	$1.00e^{-14}$	85 genes

See Supplementary Table S1 for all data.

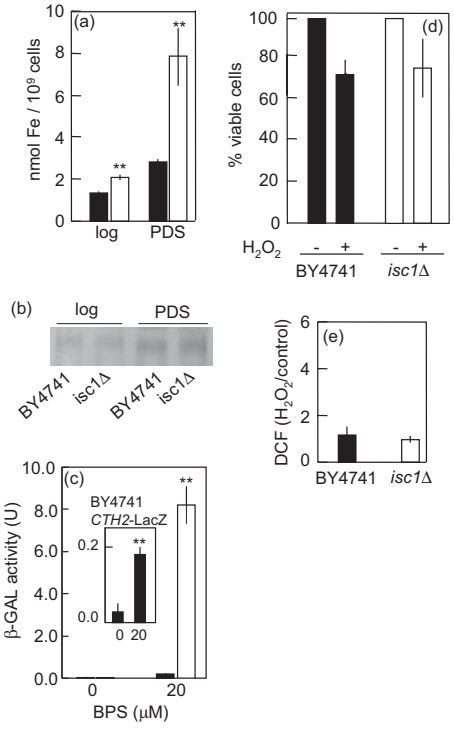

Figure 4. Iron overload contributes to oxidative stress sensitivity of Isc1p-deficient cells. *S. cerevisiae* BY4741 (■) and *isc1*Δ (□) cells were grown on YPD media to exponential (log) or postdiauxic shift (PDS) phase. (a) Iron levels were quantified as described in *Materials and Methods.* (b) Cell lysates were separated by native PAGE, and MnSOD activity was detected in situ as described in *Materials and Methods.* (c) *S. cerevisiae* BY4741 *CTH2*-LacZ (■) and *isc1*Δ *CTH2*-LacZ (□) cells, expressing the consensus Aft1 binding sequences from *CTH2* promoter fused to a LacZ reporter, were grown on minimal media to the log phase. β-galactosidase activity was measured in cells untreated or treated with BPS for 4 h. (d) H_2O_2 resistance. *S. cerevisiae* BY4741 and *isc1*Δ cells grown on YPD media to exponential phase and preincubated with 20 μM BPS for 4 h were treated with 1.5 mM H_2O_2 for 1 h. Cell viability was expressed as the percentage of the colony-forming units (H_2O_2 treated cells vs. non-stressed cells). (e) Intracellular oxidation. Cells pretreated with BPS were labeled with the molecular probe H_2DCFDA, exposed to 1.5 mM H_2O_2 for 1 h, and lysed as described in *Materials and Methods.* Data are expressed as the fluorescence ratio between H_2O_2-treated and untreated cells. Values are means ± SD of three independent experiments. $^{**}p < 0.01$.

if Isc1p deficiency activates Aft1p, both parental and *isc1*Δ mutant cells were transformed with plasmids containing the consensus (*CTH2-LacZ*) or mutant (*CTH2-LacZ* M3) Aft1 binding sequences from *CTH2* promoter fused to a LacZ reporter (Puig *et al.*, 2005). The constitutive β-galactosidase activity was similar in *isc1*Δ and the parental strain, both in exponential phase (Figure 4C) and postdiauxic phase cells (data not shown), suggesting that the induction of iron uptake genes in the mutant strain is not regulated by Aft1p. It should be noted, however, that the activation of the Aft1p reporter by treatment with the iron chelator BPS was considerably more enhanced in cells lacking Isc1p than in the parental strain (Figure 4C). As expected, β-galactosidase activity was not detected in cells transformed with the mutant (*CTH2-LacZ* M3) reporter (data not shown).

Iron is a redox active metal ion that promotes the conversion of H_2O_2 into the highly reactive hydroxyl radicals. Excess iron may therefore contribute to oxidative stress sensitivity of cells lacking Isc1p. To test this hypothesis, we analyzed the effect of the BPS on intracellular oxidation (using H_2DCFDA probe) and oxidative stress–induced cell death. Under iron deprivation conditions, H_2O_2 sensitivity and H_2O_2-induced intracellular oxidation were significantly reduced and were similar in both parental and *isc1*Δ cells (Figure 4, D and E): 70% cells remained viable and intracellular oxidation increased only twofold upon exposure to 1.5 mM H_2O_2 for 1 h (in comparison to an increase of about four- and ninefold for the parental and *isc1*Δ cells, respectively, in the absence of BPS; Figure 2). The overall results suggest that the lower resistance to H_2O_2 of cells deficient in Isc1p is associated with a higher intracellular oxidation due to iron overload.

Cells Lacking Isc1p Show Premature Ageing Associated with Oxidative Stress Markers

Ageing is characterized by the progressive loss of function over time that has been associated with the accumulation of oxidatively damaged molecules. In agreement, studies in yeast and other model organisms showed that failure to prevent oxidative damages in antioxidant-deficient cells and to repair or degrade damaged molecules reduces lifespan (Longo *et al.*, 1996, 1999; Chen *et al.*, 2004, 2005; Marques *et al.*, 2006), and the overexpression of antioxidant defenses delays aging (Sun *et al.*, 2002; Harris *et al.*, 2003, 2005). In yeast cells, chronological lifespan has been studied by measuring the capacity of postmitotic cells to maintain viability over time. The increased sensitivity of *isc1*Δ mutant cells to oxidative stress led us to investigate the role of Isc1p on chronological lifespan. Yeast cells were grown to exponential (fermentative) phase or to postdiauxic (respiratory) phase, transferred into water, and incubated at 26°C (Figure 5). In the parental strain, respiration-adapted cells displayed a longer chronological lifespan, as previously described

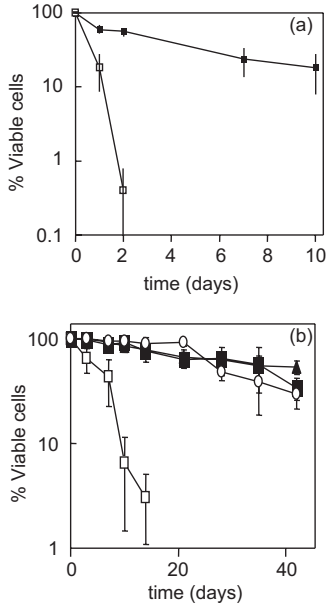

Figure 5. Isc1p deficiency decreases chronological lifespan by a Yca1p-dependent mechanism. BY4741 (■), *isc1*Δ (□), *yca1*Δ (▲) and *isc1*Δ *yca1*Δ (○) cells were grown to the exponential (a) or postdiauxic (b) phase, washed twice with H_2O, and kept in H_2O at 26°C. The viability was determined by standard dilution plate counts and expressed as the percentage of the colony-forming units at time 0 h. Data are means ± SD of three independent experiments.

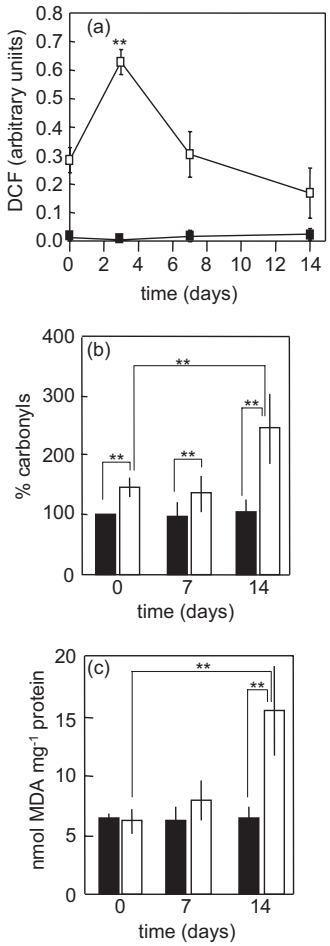

Figure 6. Intracellular oxidation and oxidative damages during chronological aging. Yeast cells were grown to postdiauxic phase, washed twice with H_2O, and kept in H_2O at 26°C. (a) Intracellular oxidation. *S. cerevisiae* BY4741 (■) and *isc1*Δ mutant (□) cells were labeled with the molecular probe H_2DCFDA and lysed as described in *Materials and Methods.* Data are expressed in arbitrary units at indicated time. (b) Protein carbonylation. Protein extracts were prepared from *S. cerevisiae* BY4741 (■) and *isc1*Δ mutant (□) cells, derivatized with DNPH and slot-blotted into a PVDF membrane. Immunodetection was performed using an anti-DNP antibody, as described in *Materials and Methods.* Quantitative analysis of total protein carbonyl content was performed by densitometry using data taken from the same membrane. (c) Lipid peroxidation. Cellular extracts were prepared and MDA was determined as described in *Materials and Methods.* Values are means ± SD of three independent experiments. **$p < 0.01$.

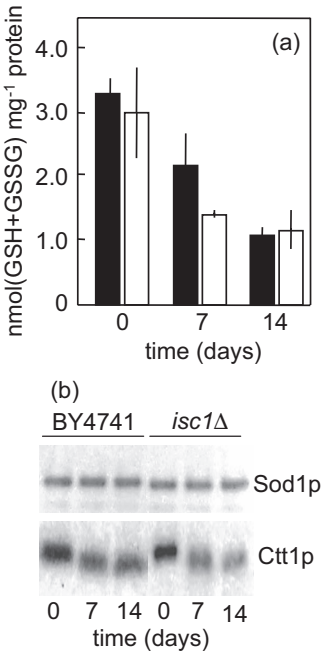

Figure 7. Antioxidant defenses during chronological aging. *S. cerevisiae* BY4741 (■) and *isc1*Δ mutant (□) cells were grown to postdiauxic phase, washed twice with H_2O, and kept in H_2O at 26°C. (a) Total glutathione levels were determined as described in *Materials and Methods.* Values are means ± SD of three independent experiments. (b) Superoxide dismutase 1 (Sod1p) and Catalase T (Ctt1p) activity. Cells were lysed and proteins were separated by native PAGE. Enzyme activity was detected as described in *Materials and Methods.* A representative experiment is shown.

(MacLean *et al.*, 2001). Yeast cells lacking Isc1p showed a premature aging phenotype: in fermentation-adapted cells, cellular viability at day 2 was 57 and 0.4% for parental and *isc1*Δ mutant cells, respectively (Figure 5A); in respiration-adapted cells, cellular viability at day 10 was 94% for parental cells and 11% for *isc1*Δ mutant cells (Figure 5B). As observed for H_2O_2 resistance, *ISC1* overexpression did not affect chronological lifespan (Supplementary Figure S2). It is possible that there is no gain of function by *ISC1* overexpression. Isc1p is regulated posttranslationaly (Vaena de Avalos *et al.*, 2004), and when endogenous Isc1p is activated, it may not be a limiting factor for ceramide generation.

We postulated that the decreased chronological lifespan of *isc1*Δ mutant cells could be associated with higher levels of oxidative stress markers. Indeed, the results showed that Isc1p deficiency increased 2.4- to 2.8-fold protein carbonylation and lipid peroxidation levels during aging of respiration-adapted cells (Figure 6). Notably, the constitutive levels of intracellular oxidation were higher in *isc1*Δ mutant cells, which are correlated with higher basal protein carbonyl content. Intracellular oxidation further increased in cells aged 3 d, but it returned to basal levels thereafter. However, during cell aging, intracellular oxidation in *isc1*Δ mutant cells was always higher than the observed in parental cells. The progressive accumulation of oxidative damaged molecules may result from an age-dependent decline in the levels of antioxidant defenses. Aiming at investigating if *ISC1* deletion exacerbated this process, we measured glutathione levels and the activity of the cytosolic superoxide dismutase and catalase. In BY4741 cells, we observed a decrease in glutathione and catalase T, but not CuZn-superoxide dismutase, during chronological aging. Similar changes were observed in *isc1*Δ cells, suggesting that the premature aging of Isc1p-deficient cells is not associated with altered levels of these antioxidant defenses (Figure 7). Interestingly, the decrease in catalase T activity was associated with a shift in the mobility of the enzyme on a native gel.

Because *isc1*Δ mutant cells contain 3–4-fold higher levels of iron (Figure 4A), and iron is known to catalyze the production of hydroxyl radicals, we raised the hypothesis that iron depletion may exert a protective effect. To test this hypothesis, *isc1*Δ mutant cells were grown overnight with 0, 20, or 100 μM BPS before the lifespan assay. Our data show that chronological lifespan was not increased by iron chelation. A dose-dependent decrease was even observed (Supplementary Figure S3). The detrimental effects of iron deple-

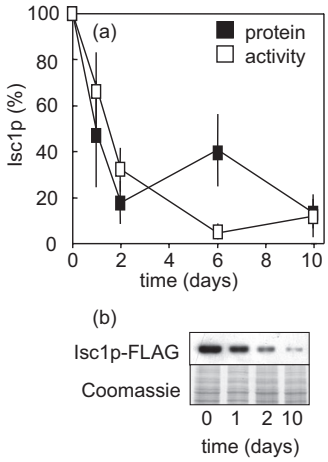

Figure 8. Isc1 specific activity and protein levels during chronological aging. (a) For Isc1p activity (□), *S. cerevisiae* BY4741 cells were grown in YPD medium to postdiauxic phase, washed twice with H_2O, and kept in H_2O at 26°C. Enzyme activity was determined as described in *Materials and Methods* and expressed as percentage of control (enzyme activity at time 0 h). For Isc1 protein levels (■), *S. cerevisiae isc1*Δ pYES2-*ISC1-FLAG* cells were grown in minimal medium with 2% galactose, washed twice with H_2O, and kept in H_2O. Proteins were isolated, separated by SDS-PAGE, and blotted into a membrane. Isc1p levels were determined by immunoblotting, using an anti-FLAG antibody, as described in *Materials and Methods*. Results were expressed as percentage of control (Isc1p level at time 0 h). Values are means ± SD. (b) A representative blot is shown (out of three independent experiments). A replica gel was stained with Coomassie blue (loading control; only a region of the gel is shown).

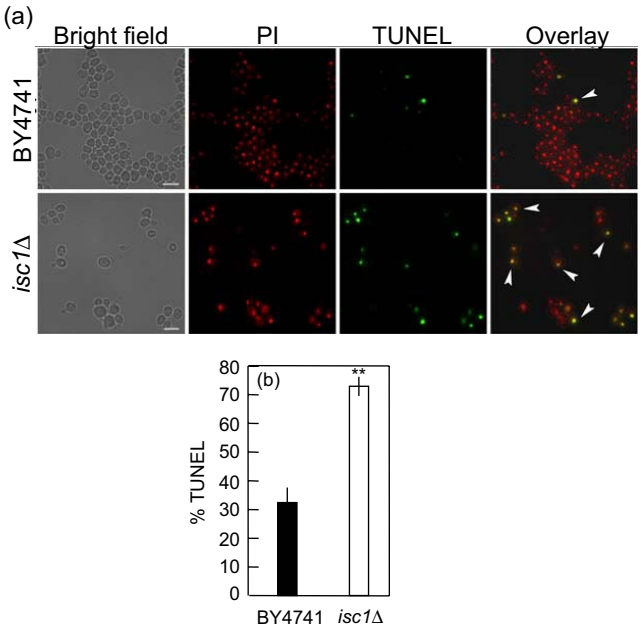

Figure 9. Apoptotic markers during oxidative stress. *S. cerevisiae* BY4741 and *isc1*Δ cells were grown to the exponential phase and treated with 1.5 mM H_2O_2 for 200 min. (a) DNA fragmentation was detected by the TUNEL assay as described in *Materials and Methods*. The nucleus was stained with PI. (b) Quantification of TUNEL-positive cells. Values are means ± SD of three independent experiments. **$p < 0.01$ (*isc1*Δ vs. BY4741). Bar, 5 μm.

tion on lifespan can be due to the fact that ATP production in aging cells is dependent on mitochondrial respiration that requires iron as part of the iron-sulfur clusters.

Isc1p Levels Decrease during Ageing

To characterize age-related changes in Isc1p, we quantified the enzyme activity and protein levels during aging of parental cells grown to postdiauxic phase. As shown in Figure 8, Isc1p specific activity decreased 70% during the first 2 d of aging, and remained at low levels (15%) up to day 10. It is unlikely that this decrease is due to oxidative inactivation, because Isc1p activity was not affected in cells treated with 1.5 mM H_2O_2 (data not shown). Changes in Isc1p protein levels were determined using yeast cells expressing a FLAG-tagged Isc1p and an anti-FLAG antibody. *S. cerevisiae isc1*Δ cells were transformed with pYES2-*ISC1-FLAG* (Vaena de Avalos *et al.*, 2004) and grown in minimal medium with 2% galactose. The results show that Isc1p protein levels decreased in aged cells at a rate similar to the observed for enzyme activity (Figure 8). The overall results indicate a correlation between cell aging and the decrease in Isc1p activity.

Isc1p Deficiency Increases Apoptosis during Oxidative Stress and Ageing

Yeast apoptosis is induced by oxidative stress and during aging (Madeo *et al.*, 1999, 2002; Fabrizio *et al.*, 2004; Herker *et al.*, 2004), and sphingolipids have been implicated in the regulation of this process in mammalian cells (Hannun and Luberto, 2000). Therefore we postulated that Isc1p deficiency might increase cell death by apoptosis. To test this hypothesis, we analyzed DNA fragmentation by the TUNEL assay in BY4741 and *isc1*Δ cells treated with H_2O_2. As shown in Figure 9, the number of TUNEL-positive *isc1*Δ cells was significantly higher (73%) compared with parental strain (32%). Under these conditions, treated unfixed cells, like untreated, remained PI negative (data not shown). The DNA fragmentation and maintenance of membrane integrity observed in *isc1*Δ mutant cells treated with H_2O_2, as observed in parental cells, support the hypothesis that these mutant cells die by apoptosis. These results were further supported by data showing that disruption of *YCA1* gene, which encodes the yeast metacaspase, in the *isc1*Δ strain increased H_2O_2 resistance to levels observed in parental cells (Figure 1A). A previous study has shown that *yca1*Δ mutant cells display a higher resistance to H_2O_2 (Madeo *et al.*, 2002). In the BY4741 background, we did not observe a higher tolerance to H_2O_2 in *yca1*Δ mutants. This may be explained by a decrease in caspase activation along cell growth in response to H_2O_2, as observed for acetic acid (Pereira *et al.*, 2007). Thus, the unperceptible effect in cell survival in absence of Yca1p only became apparent in the high sensitive isc*1*Δ mutant.

To further test the hypothesis that the loss of *ISC1* gene might accelerate the process of cell death by apoptosis, we also analyzed DNA fragmentation and caspase activity during chronological aging (Figure 10). In the parental strain, we observed an increase in TUNEL-positive cells and caspase activity with aging (Figure 10). The increase in these apoptotic markers was significantly higher in *isc1*Δ cells (Figure 10), and the premature aging of these mutants was suppressed in *isc1*Δ*yca1*Δ double mutants that lack the Yca1p metacaspase (Figure 5B). These results implicate Isc1p in the regulation of apoptotic cell death during oxidative stress and cell aging.

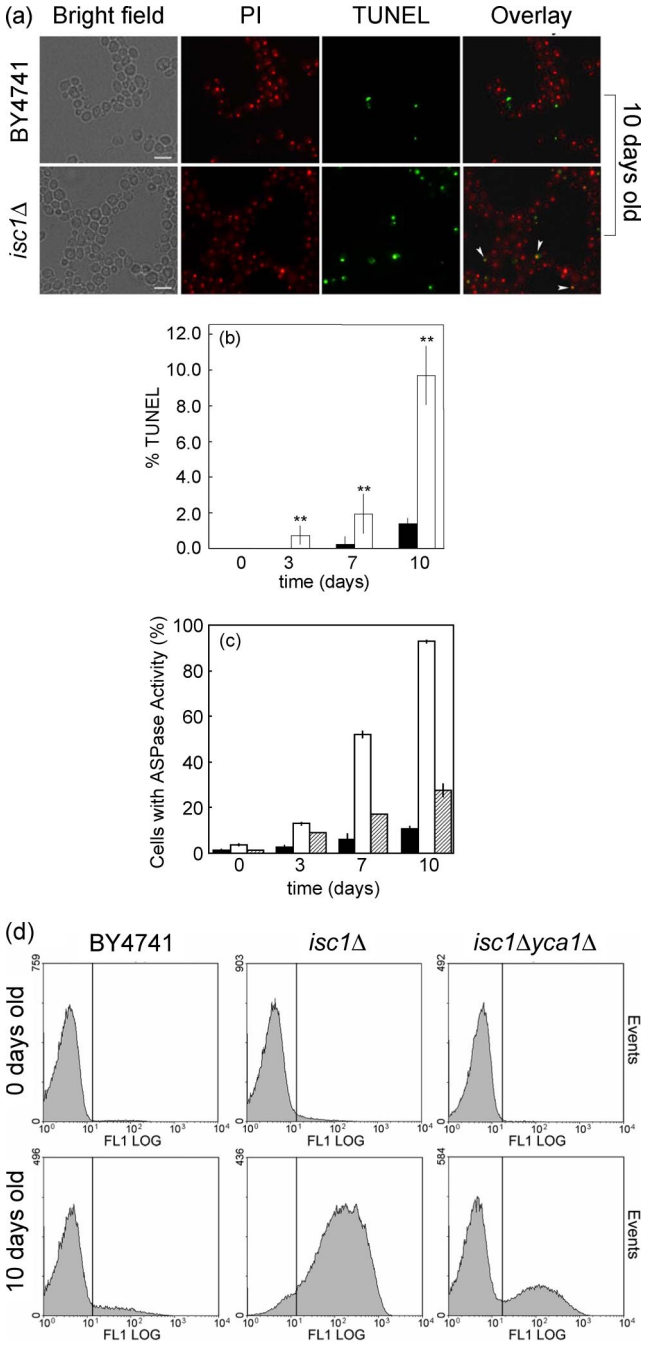

Figure 10. Apoptotic markers during chronological aging. *S. cerevisiae* BY4741 (■), *isc1*Δ (□), and *isc1*Δ*yca1*Δ (▨) cells were grown to the postdiauxic phase, washed twice with H_2O, and kept in H_2O at 26°C. (a) DNA fragmentation was detected by the TUNEL assay as described in *Materials and Methods.* The nucleus was stained with PI. (b) Quantification of TUNEL-positive cells. (c) Caspase-like or ASPase activity. Percentage of cells displaying caspase-like or ASPase activity was assessed by flow cytometric quantification of cells incubated with D_2R, as described in *Materials and Methods.* A representative experiment for control (0 d) and 10-d old cells is shown in d. Values are means ± SD of three independent experiments. **$p < 0.01$ (*isc1*Δ vs. BY4741). Bar, 5 μm.

DISCUSSION

Sphingolipids such as ceramide, sphingosine, and sphingosine-1-phosphate are important signaling molecules conserved during evolution, with roles in differentiation, senescence, cell cycle arrest, apoptosis, and stress responses (Hannun and Luberto, 2000; Ohanian and Ohanian, 2001). Data published in recent years have established a link between sphingolipid signaling and redox regulation. Sphingolipids regulate cellular redox homeostasis, and the activity of sphingomyelinases and ceramidase can be modulated by ROS and glutathione levels (Won and Singh, 2006). In *Aspergillus nidulans*, LCBs induce apoptosis associated with the accumulation of ROS, although ROS scavenging does not impair the induction of apoptosis (Cheng *et al.*, 2003). In mammalian cells, ceramide has also been shown to increase the production of ROS, by directly inhibiting the mitochondrial complex III (Gudz *et al.*, 1997) and via inhibition of Bcl2 mediated by the ceramide-activated protein phosphatase 2A (Ruvolo *et al.*, 1999). The present study showed that Isc1p, the budding yeast neutral sphingomyelinase homologue, plays a key role in oxidative stress resistance and chronological lifespan. Isc1p deficiency increased H_2O_2- and aging-induced intracellular oxidation, protein carbonylation, and lipid peroxidation. In agreement, Isc1p protects the fungus *Cryptococcus neoformans* from the oxidative stress environment of macrophages (Shea *et al.*, 2006). Interestingly, *isc1*Δ cells accumulate IPC and $M(IP)_2C$ (Sawai *et al.*, 2000), and other yeast mutants showed an inverse correlation between oxidative stress resistance or chronological lifespan and $M(IP)_2C$ levels (Aerts *et al.*, 2006). Our results support the hypothesis that $M(IP)_2C$ levels influence oxidative stress resistance and chronological lifespan in yeast. These complex IPS are yeast specific. Mammalian cells form sphingomyelin, which contains a choline group instead of the inositol moiety of yeast IPS. The expression of mouse sphingomyelin synthase increases H_2O_2 resistance in yeast cells (Yang *et al.*, 2006). Therefore, $M(IP)_2C$ and sphingomyelin may play distinct roles during oxidative stress.

Studies in yeast and other model organisms have shown a correlation between oxidative stress resistance and longevity (Sun *et al.*, 2002; Harris *et al.*, 2003, 2005; Chen *et al.*, 2004, 2005; Marques *et al.*, 2006). Our studies showed that the premature aging phenotype of *isc1*Δ cells with increased levels of oxidative stress markers was not associated with changes in antioxidant defenses. In parental cells and *isc1*Δ cells, the decrease in glutathione levels and catalase activity during aging was similar. It has been proposed that a decrease in the levels of glutathione, an inhibitor of neutral sphingomyelinases, increases sphingomyelin hydrolysis, leading to the generation of excessive amounts of ceramide (Won and Singh, 2006). Despite glutathione depletion, we observed a decrease in Isc1p activity during chronological aging of parental cells that was correlated with a reduction in protein levels.

Loss of Isc1p also did not impair the induction of genes encoding major antioxidant defenses and heat-shock proteins by exposure to sublethal H_2O_2 doses or during growth to postdiauxic phase. These results further support the lack of correlation between *isc1*Δ mutant phenotype and deficiency in stress defenses. Global changes in the transcriptome showed that carbohydrate metabolism and siderochrome transport were the most significantly overrepresented biological processes up-regulated in *isc1*Δ mutants. Microarray analysis also showed the up-regulation of genes encoding cell wall proteins. This is consistent with a previous report showing that the *S. pombe* Isc1p homologue, Ccs1p, is important for cell wall organization as it coordinates cell wall formation and division (Feoktistova *et al.*, 2001). The induction of the glycolytic pathway probably aims to compensate for a decreased production of ATP in the mitochondria, as

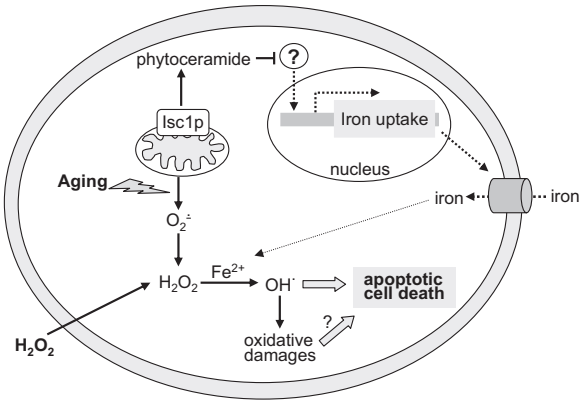

Figure 11. A model for the role of Isc1p in the regulation of iron uptake: implications during oxidative stress and cell aging. During oxidative stress induced by exogenous H_2O_2 or mitochondrial dysfunction in aged cells, iron catalyzes the conversion of H_2O_2 into hydroxyl radicals (Fenton reaction), leading to the accumulation of oxidative damages and to apoptotic cell death. Iron uptake genes are down-regulated by an Isc1p-dependent mediated pathway. In *isc1*Δ mutant cells, iron overload promotes the Fenton reaction and therefore increases apoptosis.

*isc1*Δ mutants have a decreased capacity to grow by respiration (Vaena de Avalos *et al.*, 2005). In agreement with the increased expression of four genes encoding components of the nonreductive iron uptake system (*ARN1, ARN2, ARN3,* and *ARN4*), and two genes encoding cell wall mannoproteins involved in the retention of siderophore-iron in the cell wall (*FIT2* and *FIT3*; Philpott *et al.*, 2002), iron levels increased. The intracellular localization of excess iron is an important issue to be characterized. It seems unlikely to be in the mitochondria because the accumulation of iron within this organelle was recently associated with a decrease in MnSOD activity in the yeast model of Friedreich ataxia (Irazusta *et al.*, 2006), and we did not measure any change in this antioxidant defense due to Isc1p deficiency. Iron is an essential metal ion used in iron sulfur clusters, hemes, and diiron-oxo metal clusters in enzymes. However, excess iron can promote the conversion of H_2O_2 into the highly reactive hydroxyl radicals (Halliwell and Gutteridge, 1999). The present study also showed that iron overload contributes to the hypersensitivity to H_2O_2 and to the increased levels of oxidative stress markers in *isc1*Δ cells (Figure 11). Indeed, iron deprivation significantly reduced H_2O_2 sensitivity and H_2O_2-induced intracellular oxidation in *isc1*Δ cells to the levels observed in parental cells.

The iron regulon is transcriptionally activated in response to iron deprivation by the iron-dependent transcription factors Aft1/2p (Rutherford *et al.*, 2005). Despite the constitutive up-regulation of iron uptake genes, Aft1p was not constitutively activated in *isc1*Δ mutants. In postdiauxic phase cells, iron overload was even higher, but Aft1p activity was similar in *isc1*Δ and parental cells. How lack of Isc1p induces iron accumulation remains unknown, but our results suggest that another regulator is probably involved. Interestingly, Isc1p deficiency significantly increased Aft1p activation upon iron chelation. Aft1p functions as an iron sensor responding to a signal connected to mitochondrial iron-sulfur cluster biogenesis (Rutherford *et al.*, 2005). The identification of this signal and whether it increases to higher levels in iron depleted *isc1*Δ cells is an important issue for future studies.

In response to oxidative stress and during aging, yeast cells die by an apoptotic-like and Yca1p-dependent mechanism. Yca1p exhibits proteolytic activity analogous to mammalian caspases, key proteases in the execution phase of apoptosis, and is activated by oxidative stress and aging (Madeo *et al.*, 2002). During replicative aging and in apoptotic cells, a core of genes commonly induced includes five genes in the sphingolipid metabolism functional category (Laun *et al.*, 2005). This is consistent with an unbalance in sphingolipid levels being a causing factor of apoptosis. Here, we showed that Isc1p deficiency increased H_2O_2-induced cell death and accelerated cell aging with apoptotic features: membrane integrity was maintained, DNA fragmentation increased, and the phenotype of *isc1*Δ cells was suppressed by disruption of the *YCA1* gene. In addition, caspase activation was significantly higher in *isc1*Δ aged cells.

In summary, our data show that Isc1p plays a key role in maintaining cellular redox homeostasis through modulation of iron levels. Loss of Isc1p decreased H_2O_2 resistance and chronological lifespan. In both conditions, the increased cell death was associated with apoptotic and oxidative stress markers (Figure 11). Interestingly, the neutral sphingomyelinase 2, the mammalian orthologue of Isc1p, has been implicated in H_2O_2- and TNF-induced apoptosis (Luberto *et al.*, 2002; Levy *et al.*, 2006). However, it has also been suggested that ceramides containing different fatty acids may have distinct impacts in cell physiology, by differentially affecting the biophysical properties of the membrane lipid bilayer or by interacting with specific downstream components in signaling pathways (Cutler and Mattson, 2001). The characterization of Isc1p-dependent changes in sphingolipid levels during oxidative stress and cell aging and the identification of protein targets modulated by specific sphingolipids will contribute to our understanding of the molecular mechanisms underlying oxidative stress resistance, longevity, and apoptosis.

ACKNOWLEDGMENTS

We are grateful to Professor Dennis Thiele (Duke University Medical Center, North Carolina) and Professor Yusuf Hannun (Medical University of South Carolina) for helpful suggestions and for generously providing plasmids used in this study. This project was financially supported by FCT, POCTI/BCI/45066/2002, and FSE-FEDER. T.A. and M.M. were supported by FCT BD fellowships.

REFERENCES

Abramova, N. E., Cohen, B. D., Sertil, O., Kapoor, R., Davies, K. J., and Lowry, C. V. (2001). Regulatory mechanisms controlling expression of the DAN/TIR mannoprotein genes during anaerobic remodeling of the cell wall in *Saccharomyces cerevisiae.* Genetics *157*, 1169–1177.

Aerts, A. M., Francois, I. E., Bammens, L., Cammue, B. P., Smets, B., Winderickx, J., Accardo, S., De Vos, D. E., and Thevissen, K. (2006). Level of $M(IP)_2C$ sphingolipid affects plant defensin sensitivity, oxidative stress resistance and chronological life-span in yeast. FEBS Lett. *580*, 1903–1907.

Almeida, B., Sampaio-Marques, B., Carvalho, J., Silva, M. T., Leao, C., Rodrigues, F., and Ludovico, P. (2007). An atypical active cell death process underlies the fungicidal activity of ciclopirox olamine against the yeast *Saccharomyces cerevisiae.* FEMS Yeast Res. *7*, 404–412.

Ausubel, F. A., Brent, R., Kingston, D., Moore, D., Seidman, J. G., Smith J. A., and Struhl, K. (1998). Current Protocols in Molecular Biology, New York: John Wiley and Sons.

Belinha, I., Amorim, M. A., Rodrigues, P., de Freitas, V., Moradas-Ferreira, P., Mateus, N., and Costa, V. (2007). Quercetin increases oxidative stress resistance and longevity in *Saccharomyces cerevisiae.* J. Agric. Food Chem. *55*, 2446–2451.

Cabiscol, E., Piulats, E., Echave, P., Herrero, E., and Ros, J. (2000). Oxidative stress promotes specific protein damage in *Saccharomyces cerevisiae*. J. Biol. Chem. *275*, 27393–27398.

Chen, Q., Ding, Q., Thorpe, J., Dohmen, R. J., and Keller, J. N. (2005). RNA interference toward UMP1 induces proteasome inhibition in *Saccharomyces cerevisiae*: evidence for protein oxidation and autophagic cell death. Free Radic. Biol. Med. *38*, 226–234.

Chen, Q., Thorpe, J., Ding, Q., El-Amouri, I. S., and Keller, J. N. (2004). Proteasome synthesis and assembly are required for survival during stationary phase. Free Radic. Biol. Med. *37*, 859–868.

Cheng, J., Park, T. S., Chio, L. C., Fischl, A. S., and Ye, X. S. (2003). Induction of apoptosis by sphingoid long-chain bases in *Aspergillus nidulans*. Mol. Cell. Biol. *23*, 163–177.

Conyers, S. M., and Kidwell, D. A. (1991). Chromogenic substrates for horseradish peroxidase. Anal. Biochem. *192*, 207–211.

Costa, V., and Moradas-Ferreira, P. (2001). Oxidative stress and signal transduction in *Saccharomyces cerevisiae*: insights into ageing, apoptosis and diseases. Mol. Aspects Med. *22*, 217–246.

Costa, V. M., Amorim, M. A., Quintanilha, A., and Moradas-Ferreira, P. (2002). Hydrogen peroxide-induced carbonylation of key metabolic enzymes in *Saccharomyces cerevisiae*: the involvement of the oxidative stress response regulators Yap1 and Skn7. Free Radic. Biol. Med. *33*, 1507–1515.

Cowart, L. A., Okamoto, Y., Lu, X., and Hannun, Y. A. (2006). Distinct roles for de novo versus hydrolytic pathways of sphingolipid biosynthesis in *Saccharomyces cerevisiae*. Biochem. J. *393*, 733–740.

Cutler, R. G., and Mattson, M. P. (2001). Sphingomyelin and ceramide as regulators of development and lifespan. Mech. Ageing Dev. *122*, 895–908.

Davidson, J. F., Whyte, B., Bissinger, P. H., and Schiestl, R. H. (1996). Oxidative stress is involved in heat-induced cell death in *Saccharomyces cerevisiae*. Proc. Natl. Acad. Sci. USA *93*, 5116–5121.

Desmyter, L., Dewaele, S., Reekmans, R., Nystrom, T., Contreras, R., and Chen, C. (2004). Expression of the human ferritin light chain in a frataxin mutant yeast affects ageing and cell death. Exp. Gerontol. *39*, 707–715.

Destruelle, M., Holzer, H., and Klionsky, D. J. (1994). Identification and characterization of a novel yeast gene: the YGP1 gene product is a highly glycosylated secreted protein that is synthesized in response to nutrient limitation. Mol. Cell. Biol. *14*, 2740–2754.

Fabrizio, P., Battistella, L., Vardavas, R., Gattazzo, C., Liou, L. L., Diaspro, A., Dossen, J. W., Gralla, E. B., and Longo, V. D. (2004). Superoxide is a mediator of an altruistic aging program in *Saccharomyces cerevisiae*. J. Cell Biol. *166*, 1055–1067.

Feoktistova, A., Magnelli, P., Abeijon, C., Perez, P., Lester, R. L., Dickson, R. C., and Gould, K. L. (2001). Coordination between fission yeast glucan formation and growth requires a sphingolipase activity. Genetics *158*, 1397–1411.

Flohé, L., and Otting, F. (1984). Superoxide dismutase assays. Methods Enzymol. *105*, 93–104.

Godon, C., Lagniel, G., Lee, J., Buhler, J. M., Kieffer, S., Perrot, M., Boucherie, H., Toledano, M. B., and Labarre, L. (1998). The H_2O_2 stimulon in *Saccharomyces cerevisiae*. J. Biol. Chem. *273*, 22480–22489.

Gudz, T. I., Tserng, K. Y., and Hoppel, C. L. (1997). Direct inhibition of mitochondrial respiratory chain complex III by cell-permeable ceramide. J. Biol. Chem. *272*, 24154–24158.

Halliwell, B., and Gutteridge, J.M.C. (1999). Free Radicals in Biology and Medicine, 3rd ed., London: Oxford University Press.

Hannun, Y. A., and Luberto, C. (2000). Ceramide in the eukaryotic stress response. Trends Cell Biol. *10*, 73–80.

Harris, N., Bachler, M., Costa, V., Mollapour, M., Moradas-Ferreira, P., and Piper, P. W. (2005). Overexpressed Sod1p acts either to reduce or to increase the lifespans and stress resistance of yeast, depending on whether it is Cu(2+)-deficient or an active Cu, Zn-superoxide dismutase. Aging Cell *4*, 41–52.

Harris, N., Costa, V., MacLean, M., Mollapour, M., Moradas-Ferreira, P., and Piper, P. W. (2003). Mnsod overexpression extends the yeast chronological (G(0)) life span but acts independently of Sir2p histone deacetylase to shorten the replicative life span of dividing cells. Free Radic. Biol. Med. *34*, 1599–1606.

Herker, E., Jungwirth, H., Lehmann, K. A., Maldener, C., Fröhlich, K. U., Wissing, S., Büttner, S., Fehr, M., Sigrist, S., and Madeo, F. (2004). Chronological aging leads to apoptosis in yeast. J. Cell Biol. *164*, 501–507.

Inai, Y., and Nishikimi, M. (2002). Increased degradation of oxidized proteins in yeast defective in 26 S proteasome assembly. Arch. Biochem. Biophys. *404*, 279–284.

Irazusta, V., Cabiscol, E., Reverter-Branchat, G., Ros, J., and Tamarit, J. (2006). Manganese is the link between frataxin and iron-sulfur deficiency in the yeast model of Friedreich ataxia. J. Biol. Chem. *281*, 12227–12232.

Jenkins, G. M., Cowart, L. A., Signorelli, P., Pettus, B. J., Chalfant, C. E., and Hannun, Y. A. (2002). Acute activation of de novo sphingolipid biosynthesis upon heat shock causes an accumulation of ceramide and subsequent dephosphorylation of SR proteins. J. Biol. Chem. *277*, 42572–42578.

Jiang, J. C., Kirchman, P. A., Allen, M., and Jazwinski, S. M. (2004). Suppressor analysis points to the subtle role of the LAG1 ceramide synthase gene in determining yeast longevity. Exp. Gerontol. *39*, 999–1009.

Kosman, D. J. (2003). Molecular mechanisms of iron uptake in fungi. Mol. Microbiol. *47*, 1185–1197.

Laun, P. *et al.* (2005). A comparison of the aging and apoptotic transcriptome of *Saccharomyces cerevisiae*. FEMS Yeast Res. *5*, 1261–1272.

Le Stunff, H., Peterson, C., Liu, H., Milstien, S., and Spiegel, S. (2002). Sphingosine-1-phosphate and lipid phosphohydrolases. Biochim. Biophys. Acta *1582*, 8–17.

Levy, M., Castillo, S. S., and Goldkorn, T. (2006). nSMase2 activation and trafficking are modulated by oxidative stress to induce apoptosis. Biochem. Biophys. Res. Commun. *344*, 900–905.

Longo, V. D., Gralla, E. B., and Valentine, J. S. (1996). Superoxide dismutase activity is essential for stationary phase survival in *Saccharomyces cerevisiae*. Mitochondrial production of toxic oxygen species in vivo. J. Biol. Chem. *271*, 12275–12280.

Longo, V. D., Liou, L. L., Valentine, J. S., and Gralla, E. B. (1999). Mitochondrial superoxide decreases yeast survival in stationary phase. Arch. Biochem. Biophys. *365*, 131–142.

Luberto, C., Hassler, D. F., Signorelli, P., Okamoto, Y., Sawai, H., Boros, E., Hazen-Martin, D. J., Obeid, L. M., Hannun, Y. A., and Smith, G. K. (2002). Inhibition of tumor necrosis factor-induced cell death in MCF7 by a novel inhibitor of neutral sphingomyelinase. J. Biol. Chem. *277*, 41128–41139.

Ludovico, P., Sousa, M. J., Silva, M. T., Leao, C., and Corte-Real, M. (2001). *Saccharomyces cerevisiae* commits to a programmed cell death process in response to acetic acid. Microbiology *147*, 2409–2415.

MacLean, M., Harris, N., and Piper, P. W. (2001). Chronological lifespan of stationary phase yeast cells; a model for investigating the factors that might influence the ageing of postmitotic tissues in higher organisms. Yeast *18*, 499–509.

Madeo, F., Fröhlich, E., Ligr, M., Grey, M., Sigrist, S. J., Wolf, D. H., and Fröhlich, K. U. (1999). Oxygen stress: a regulator of apoptosis in yeast. J. Cell Biol. *145*, 757–767.

Madeo, F., Engelhardt, S., Herker, E., Lehmann, N., Maldener, C., Proksch, A., Wissing, S., and Frohlich, K. U. (2002). Apoptosis in yeast: a new model system with applications in cell biology and medicine. Curr. Genet. *41*, 208–216.

Mamnun, Y. M., Schuller, C., and Kuchler, K. (2004). Expression regulation of the yeast PDR5 ATP-binding cassette (ABC) transporter suggests a role in cellular detoxification during the exponential growth phase. FEBS Lett. *559*, 111–117.

Marques, M., Mojzita, D., Amorim, M. A., Almeida, T., Hohmann, S., Moradas-Ferreira, P., and Costa, V. (2006). The Pep4p vacuolar proteinase contributes to the turnover of oxidized proteins but PEP4 overexpression is not sufficient to increase chronological lifespan in *Saccharomyces cerevisiae*. Microbiology *152*, 3595–3605.

Ohanian, J., and Ohanian, V. (2001). Sphingolipids in mammalian cell signalling. Cell. Mol. Life Sci. *58*, 2053–2068.

Ojeda, L., Keller, G., Muhlenhoff, U., Rutherford, J. C., Lill, R., and Winge, D. R. (2006). Role of glutaredoxin-3 and glutaredoxin-4 in the iron regulation of the Aft1 transcriptional activator in *Saccharomyces cerevisiae*. J. Biol. Chem. *281*, 17661–17669.

Okamoto, Y., Vaena De Avalos, S., and Hannun, Y. A. (2002). Structural requirements for selective binding of ISC1 to anionic phospholipids. J. Biol. Chem. *277*, 46470–46477.

Ostrander, D. B., Zhang, M., Mileykovskaya, E., Rho, M., and Dowhan, W. (2001). Lack of mitochondrial anionic phospholipids causes an inhibition of translation of protein components of the electron transport chain. A yeast genetic model system for the study of anionic phospholipid function in mitochondria. J. Biol. Chem. *276*, 25262–25272.

Parkinson, H. *et al.* (2005). ArrayExpress—a public repository for microarray gene expression data at the EBI. Nucleic Acids Res. *33*(Database issue), D553–D555.

Pereira, C., Camougrand, N., Manon, S., Sousa, M. J., and Côrte-Real, M. (2007). ADP/ATP carrier is required for mitochondrial outer membrane per-

meabilization and cytochrome c release in yeast apoptosis. Mol. Microbiol. *66*, 571–582.

Philpott, C. C., Protchenko, O., Kim, Y. W., Boretsky, Y., and Shakoury-Elizeh, M. (2002). The response to iron deprivation in *Saccharomyces cerevisiae*: expression of siderophore-based systems of iron uptake. Biochem. Soc. Trans. *30*, 698–702.

Puig, S., Askeland, E., and Thiele, D. J. (2005). Coordinated remodeling of cellular metabolism during iron deficiency through targeted mRNA degradation. Cell *120*, 99–110.

Rep, M., Krantz, M., Thevelein, J. M., and Hohmann, S. (2000). The transcriptional response of *Saccharomyces cerevisiae* to osmotic shock. Hot1p and Msn2p/Msn4p are required for the induction of subsets of high osmolarity glycerol pathway-dependent genes. J. Biol. Chem. *275*, 8290–8300.

Robinson, M. D., Grigull, J., Mohammad, N., and Hughes, T. R. (2002). FunSpec: a web-based cluster interpreter for yeast. BMC Bioinformatics *3*, 35.

Rutherford, J. C., Ojeda, L., Balk, J., Muhlenhoff, U., Lill, R., and Winge, D. R. (2005). Activation of the iron regulon by the yeast Aft1/Aft2 transcription factors depends on mitochondrial but not cytosolic iron-sulfur protein biogenesis. J. Biol. Chem. *280*, 10135–10140.

Ruvolo, P. P., Deng, X., Ito, T., Carr, B. K., and May, W. S. (1999). Ceramide induces Bcl2 dephosphorylation via a mechanism involving mitochondrial PP2A. J. Biol. Chem. *274*, 20296–20300.

Sambrook, J., Fritsch, E. F., and Maniatis, T. (1989). Molecular Cloning: A Laboratory Manual, 2nd ed., New York: Cold Spring Harbor Laboratory.

Sawai, H., Okamoto, Y., Luberto, C., Mao, C., Bielawska, A., Domae, N., and Hannun, Y. A. (2000). Identification of ISC1 (YER019w) as inositol phosphosphingolipid phospholipase C in *Saccharomyces cerevisiae*. J. Biol. Chem. *275*, 39793–39798.

Shea, J. M., Kechichian, T. B., Luberto, C., and Del Poeta, M. (2006). The cryptococcal enzyme inositol phosphosphingolipid-phospholipase C confers resistance to the antifungal effects of macrophages and promotes fungal dissemination to the central nervous system. Infect. Immun. *74*, 5977–5988.

Shringarpure, R., Grune, T., Mehlhase, J., and Davies, K. J. (2003). Ubiquitin conjugation is not required for the degradation of oxidized proteins by proteasome. J. Biol. Chem. *278*, 311–318.

Sun, J., Folk, D., Bradley, T. J., and Tower, J. (2002). Induced overexpression of mitochondrial Mn-superoxide dismutase extends the life span of adult *Drosophila melanogaster*. Genetics *161*, 661–672.

Tamarit, J., Irazusta, V., Moreno-Cermeno, A., and Ros, J. (2006). Colorimetric assay for the quantitation of iron in yeast. Anal. Biochem. *351*, 149–151.

Tietze, F. (1969). Enzymic method for quantitative determination of nanogram amounts of total and oxidized glutathione: applications to mammalian blood and other tissues. Anal. Biochem. *27*, 502–522.

Vaena de Avalos, S., Okamoto, Y., and Hannun, Y. A. (2004). Activation and localization of inositol phosphosphingolipid phospholipase C, Isc1p, to the mitochondria during growth of *Saccharomyces cerevisiae*. J. Biol. Chem. *279*, 11537–11545.

Vaena de Avalos, S., Su, X., Zhang, M., Okamoto, Y., Dowhan, W., and Hannun, Y. A. (2005). The phosphatidylglycerol/cardiolipin biosynthetic pathway is required for the activation of inositol phosphosphingolipid phospholipase C, Isc1p, during growth of *Saccharomyces cerevisiae*. J. Biol. Chem. *280*, 7170–7177.

Won, J. S., and Singh, I. (2006). Sphingolipid signaling and redox regulation. Free Radic. Biol. Med. *40*, 1875–1888.

Yang, Z., Khoury, C., Jean-Baptiste, G., and Greenwood, M. T. (2006). Identification of mouse sphingomyelin synthase 1 as a suppressor of Bax-mediated cell death in yeast. FEMS Yeast Res. *6*, 751–762.